Chapter 7
Use of VFM for Heterogeneity Evaluation of Materials Under Uniaxial Tensile Stress

John Considine, F. Pierron, and K.T. Turner

Abstract Identification of spatially varying stiffness is a challenging, but important, research topic especially as materials become more complex and are used in extreme environments. Examination of heterogeneity is often accomplished by unique test fixtures capable of creating the necessary stress configurations for heterogeneous stiffness identification. In this work the Virtual Fields Method (VFM) was used to identify stiffnesses in a simple geometry, namely uniaxial tension, of a simulated material with an inclusion whose stiffness gradually increases from that of surrounding material. Three different VFM analyses were examined and their results compared. Results suggest that cooperative use of these analyses could provide reasonable stiffness identification for heterogeneous materials using uniaxial tensile tests.

Keywords VFM • Stiffness • Heterogeneity • Simulation • Uniaxial tension

7.1 Introduction

Identification of material stiffness is the most frequent use of the Virtual Fields Method (VFM) [1]. A common assumption within VFM is material homogeneity. Often this assumption is quite reasonable, when stiffness spatial variation is small compared to the mean stiffness. Efforts to accurately identify stiffness heterogeneity generally require non-standard test fixtures to activate sufficient full-field strains for numerical analysis. This work examines the common uniaxial tensile test and provides an overview of the use of VFM for heterogeneous stiffness identification.

The objective of this work is to summarize VFM procedures used in heterogeneous stiffness identification, along with the some of their advantages and limitations. VFM procedures can be used cooperatively to provide information on the location and size of heterogeneities. Additionally, we hope to encourage those new to, or just beginning with, VFM to understand its potential usefulness.

Characterization of material heterogeneity is important in process control in order to evaluate and maintain material quality, and in end use environments, to determine stiffness changes due to temperature, moisture, damage, or other external factors. In both occurrences initial assessment of heterogeneity may be physical, e.g., the material looks damaged in a particular location, or another tool, such as ultrasonic evaluation, may be used.

Although challenging in practice, spatially varying stiffness identification can provide an additional tool to examine the extent of material heterogeneity in terms of location(s), frequency, and stiffness gradient. The challenge for the evaluator is coordinated selection of test geometry, stiffness parameterization and appropriate inverse analysis.

The uniaxial tensile test is one of the most used test configurations for mechanical characterization. The test is quick, intuitive, and a part of many quality control processes. With the addition of full-field displacement measurements, such as digital image correlation or the grid optical technique, the uniaxial test and VFM can provide an evaluation of stiffness heterogeneity.

J. Considine (✉)
U.S. Forest Service, Forest Products Laboratory, One Gifford Pinchot Drive, Madison, WI 53726, USA
e-mail: jconsidine@fs.fed.us

F. Pierron
University of Southampton, Southampton SO17 1BJ, UK

K.T. Turner
University of Pennsylvania, 245 Towne Building, 220 S. 33rd St, Philadelphia, PA 19104-6315, USA

© The Society for Experimental Mechanics, Inc. 2016

C. Sciammarella et al. (eds.), *Experimental and Applied Mechanics, Volume 4*,
Conference Proceedings of the Society for Experimental Mechanics Series, DOI 10.1007/978-3-319-22449-7_7

Here a strip of simulated material, 25 mm × 150 mm, containing a single inclusion with smoothly varying stiffness, under uniaxial tension, was examined with three VFM techniques. Effectiveness of each identification technique was determined by comparison with known stiffness. Given that the uniaxial tensile geometry is not an optimal choice for heterogeneous material evaluation, reasonable identification was achieved.

7.2 Uniaxial Model

A thin rectangular specimen of size $L_1 \times L_2 = 150$ mm × 25 mm and thickness 1 mm was modeled in ANSYS® (ANSYS, Inc, Canonsburg, PA 15317, USA) using 3750 1 mm^2 PLANE42 elements. Origin of the coordinate system was located on the lower left of the specimen as shown in Fig. 7.1. Stiffness was smoothly varying in both the x_1- and x_2-directions and was rotated 60° with respect to x_1-direction. Attributes of the inclusion were selected to simulate actual scenarios and to challenge stiffness identification techniques. Formula for Q_{11} (GPa) is given in Eq. (7.1) and is based upon a 2-D probability curve. Poisson's Ratio was set to 0.3 throughout the model. Although any smoothly varying stiffness distribution could have been selected, those made up of $\cos(\omega x_i)$ and $\sin(\omega x_i)$ terms were intentionally excluded because one of the identification techniques is based upon Fourier transforms.

$$Q_{11} = 11.0 + 3.3e^{-(((x_1-75)*\cos(\pi/3)+(x_2-12.5)*\sin(\pi/6))/150*12)^2-(((x_1-75)*\cos(\pi/3)+(x_2-12.5)*\sin(\pi/6))/25*12)^2} \tag{7.1}$$

Figure 7.2 gives the finite element (FE) strains and those from a grid–measurement simulation. Grid simulation is described in [2]. Zero-mean, random gray scale noise was added to the simulated deformed grid image at 1 % of gray scale.

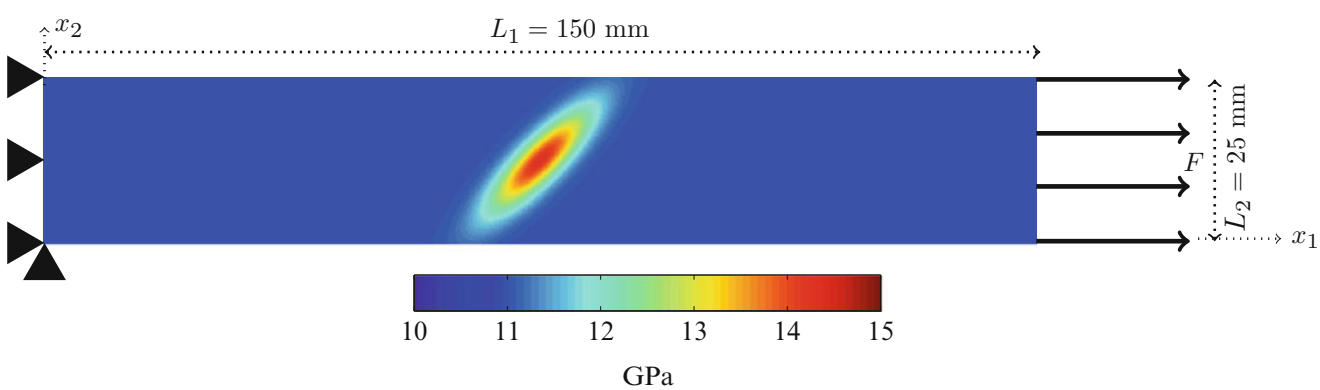

Fig. 7.1 Q_{11} for uniaxial tension model

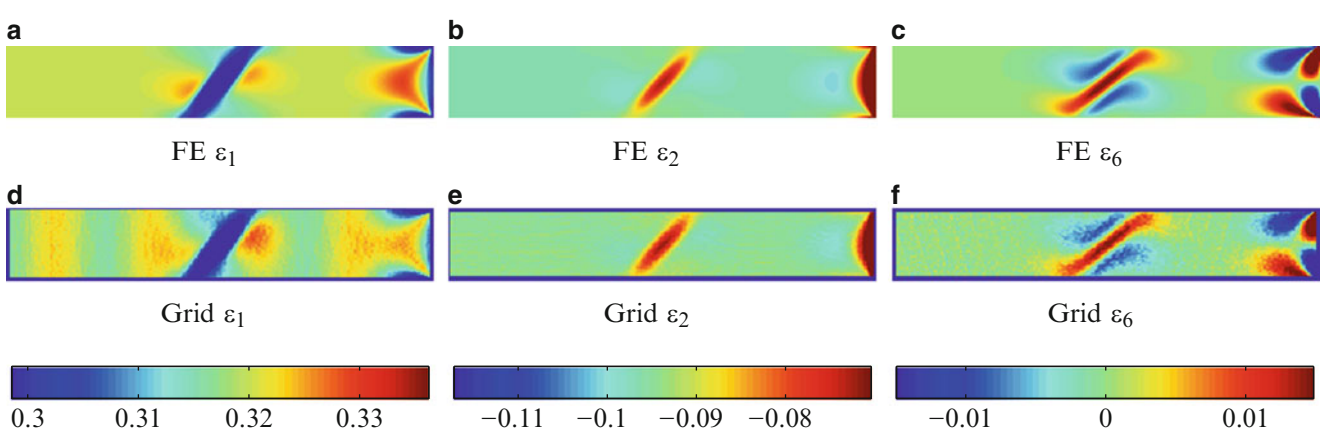

Fig. 7.2 FE strains (**a**)–(**b**) and simulated grid strains (**d**)–(**f**); scale is (%) strain. (**a**) FE ε_1. (**b**) FE ε_2. (**c**) FE ε_6. (**d**) Grid ε_1. (**e**) Grid ε_2. (**f**) Grid ε_6

7.3 Application of VFM to Heterogeneous Materials

Three VFM analyses are presented for the purpose of heterogeneity characterization. The Principle of Virtual Work (PVW) provides the basis for use of VFM to examine heterogeneous materials. For a plane stress problem, PVW can be written as

$$\int_S \left(\sigma_1 \varepsilon_1^* + \sigma_2 \varepsilon_2^* + \sigma_6 \varepsilon_6^*\right) dS = \int_{L_f} \overline{T}_i u_i^* \, dl, \tag{7.2}$$

where S is the area of 2-D domain, σ_i are stresses within S, u_i^* are kinematically admissible virtual displacements, ε_i^* are virtual strains associated with u_i^*, $\overline{T}_i$ are tractions applied on boundary of S, and L_f is the portion of S over which $\overline{T}_i$ are applied.

Assuming a linear elastic isotropic material, the constitutive equation is given by

$$\begin{Bmatrix} \sigma_1 \\ \sigma_2 \\ \sigma_6 \end{Bmatrix} = \begin{bmatrix} Q_{11} & Q_{12} & 0 \\ Q_{12} & Q_{11} & 0 \\ 0 & 0 & \dfrac{Q_{11} - Q_{12}}{2} \end{bmatrix} \begin{Bmatrix} \varepsilon_1 \\ \varepsilon_2 \\ \varepsilon_6 \end{Bmatrix} \tag{7.3}$$

Using Eq. (7.3) in Eq. (7.2) gives an experimentally useful PVW equation as

$$\int_S Q_{11}\left(\varepsilon_1 \varepsilon_1^* + \varepsilon_2 \varepsilon_2^* + \frac{1}{2}\varepsilon_6 \varepsilon_6^*\right) dS + \int_S Q_{12}\left(\varepsilon_1 \varepsilon_2^* + \varepsilon_2 \varepsilon_1^* - \frac{1}{2}\varepsilon_6 \varepsilon_6^*\right) dS = \int_{L_f} \overline{T}_i u_i^* \, dl \tag{7.4}$$

Equation (7.4) is useful because in many test systems the full-field strains, ε_i, and the external loads, $\overline{T}_i$, are measured. The contribution of VFM is the advantageous selection of the virtual fields, u_i^*, and by strain–displacement relations the virtual strains, ε_i^*, so that the stiffnesses, Q_{ij}, are determined to ensure equilibrium of S.

7.3.1 *Optimized, Piecewise Virtual Fields*

VFM has many advantages over other inverse methods, and many of those advantages are evolved from optimized, piecewise virtual fields that are used to specify the $u_i{}^*$. Two of the three VFM techniques described here use them. Virtual meshes are not dense for homogeneous materials; density is specified based on the number of stiffnesses to be identified and expected stiffness gradient. Generally, mesh density is specified such that the number of interior virtual nodes are 2× the number of stiffness values needed, but a dense mesh is used here to reduce the effects of smoothing performed by the virtual fields. The virtual mesh is shown in Fig. 7.3 where each virtual element is 5 mm × 5 mm. A detailed derivation of optimized, piecewise virtual fields is given in Sects. 3.6 and 3.7 of Pierron and Grédiac [1].

7.3.2 *Location of Inclusion Known a Priori*

Assume that the region S in Eq. (7.4) contains an inclusion whose location and boundaries are known. If $S = S_1 \cap S_2$, where S_2 is the inclusion region and S_1 is all of S outside S_2, then Eq. (7.4) can be rewritten as

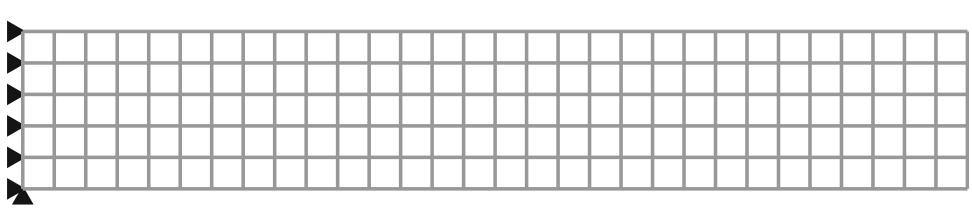

Fig. 7.3 Piecewise virtual field mesh

$$\begin{aligned}&\int_{S_1} Q_{11}^{S_1}\left(\varepsilon_1\varepsilon_1^* + \varepsilon_2\varepsilon_2^* + \frac{1}{2}\varepsilon_6\varepsilon_6^*\right)dS_1 + \int_{S_1} Q_{12}^{S_1}\left(\varepsilon_1\varepsilon_2^* + \varepsilon_2\varepsilon_1^* - \frac{1}{2}\varepsilon_6\varepsilon_6^*\right)dS_1 + \cdots \\ &+\cdots \int_{S_2} Q_{11}^{S_2}\left(\varepsilon_1\varepsilon_1^* + \varepsilon_2\varepsilon_2^* + \frac{1}{2}\varepsilon_6\varepsilon_6^*\right)dS_2 + \int_{S_2} Q_{12}^{S_2}\left(\varepsilon_1\varepsilon_2^* + \varepsilon_2\varepsilon_1^* - \frac{1}{2}\varepsilon_6\varepsilon_6^*\right)dS_2 = \int_{L_f} \overline{T}_i u_i^* dl\end{aligned} \tag{7.5}$$

Accordingly, if k inclusions exist within S, then the left-hand side of Eq. (7.5) would contain $k + 1$ integral terms, where the + 1 refers to the region not contained in the inclusions, i.e., the matrix material. For simplicity, the following development will assume only a single inclusion, but the development for multiple inclusions is straightforward.

If S_1 and S_2 are assumed to be comprised of different linear elastic isotropic materials, then Q_{ij} are constants and can be placed outside the integrals in Eq. (7.5). The new equilibrium equation is

$$\begin{aligned}&Q_{11}^{S_1}\int_{S_1}\left(\varepsilon_1\varepsilon_1^* + \varepsilon_2\varepsilon_2^* + \frac{1}{2}\varepsilon_6\varepsilon_6^*\right)dS_1 + Q_{12}^{S_1}\int_{S_1}\left(\varepsilon_1\varepsilon_2^* + \varepsilon_2\varepsilon_1^* - \frac{1}{2}\varepsilon_6\varepsilon_6^*\right)dS_1 + \cdots \\ &+\cdots Q_{11}^{S_2}\int_{S_2}\left(\varepsilon_1\varepsilon_1^* + \varepsilon_2\varepsilon_2^* + \frac{1}{2}\varepsilon_6\varepsilon_6^*\right)dS_2 + Q_{12}^{S_2}\int_{S_2}\left(\varepsilon_1\varepsilon_2^* + \varepsilon_2\varepsilon_1^* - \frac{1}{2}\varepsilon_6\varepsilon_6^*\right)dS_2 = \int_{L_f} \overline{T}_i u_i^* dl\end{aligned} \tag{7.6}$$

Although no limit on the number of S_k exists, $Q_{ij}^{S_k}$ identification requires sufficient strain data, ε_i, for each region. Practical experience has shown unstable identification for $k > 5$ [3]. Furthermore, inclusion boundaries are rarely "sharp"; an inclusion boundary layer usually exists in which stiffness gradually changes from the matrix to the inclusion. Some judgment by the analyst is needed to define the boundary contour. Conservative use of Eq. (7.6) for multiple inclusions requires that each inclusion be allowed to have unique Q_{ij} initially.

7.3.3 Equilibrium Gap

A further development in the virtual fields method [4] comes from the understanding that PVW can also be used to examine local equilibrium. A similar procedure has been used to examine errors in FE modeling [5]. Discrepancies in local equilibrium are "equilibrium gaps" (EGs) and can be used to locate boundaries of regions that are not in equilibrium with each other when material homogeneity is assumed.

Equation (7.4) can be written as

$$Q_{11}\int_{S_\gamma}\left(\varepsilon_1\varepsilon_1^* + \varepsilon_2\varepsilon_2^* + \frac{1}{2}\varepsilon_6\varepsilon_6^*\right)dS_\gamma + Q_{12}\int_{S\gamma}\left(\varepsilon_1\varepsilon_2^* + \varepsilon_2\varepsilon_1^* - \frac{1}{2}\varepsilon_6\varepsilon_6^*\right)dS_\gamma - \int_{L_f} \overline{T}_i u_i^* dl = 0 \tag{7.7}$$

Equation (7.7) describes the equilibrium of a region S_γ, where S_γ is a portion of a larger region. If all Q_{ij} are known, usually by identification by homogeneous VFM, and u^* are kinematically admissible, then summation of the integrals should be zero; a non-zero result is termed to be an equilibrium gap. In practice, $\overline{T}_i$ are zero.

7.3.4 Fourier-VFM

A recent contribution to VFM is the solution of the PVW equation (Eq. (7.4) in the frequency domain) by means of Fourier analysis.

The spatially varying Q_{ij} are represented as

$$Q_{11}(x_1,x_2) = \sum_{m=0}^{N}\sum_{n=-N}^{N} a_{m,n}\cos 2\pi\left(\frac{mx_1}{L_1}+\frac{nx_2}{L_2}\right) + \sum_{m=0}^{N}\sum_{\substack{n=-N\\ m+|n|\neq 0}}^{N} b_{m,n}\sin 2\pi\left(\frac{mx_1}{L_1}+\frac{nx_2}{L_2}\right) \tag{7.8}$$

$$Q_{12}(x_1,x_2) = \sum_{m=0}^{N}\sum_{n=-N}^{N} f_{m,n}\cos 2\pi\left(\frac{mx_1}{L_1}+\frac{nx_2}{L_2}\right) + \sum_{m=0}^{N}\sum_{\substack{n=-N\\ m+|n|\neq 0}}^{N} g_{m,n}\sin 2\pi\left(\frac{mx_1}{L_1}+\frac{nx_2}{L_2}\right) \tag{7.9}$$

Instead of using optimized, piecewise virtual fields described earlier, the virtual fields are unit amplitude sine/cosine waves. A thorough description of this technique is provided by Nguyen et al. [6].

7.4 Results and Discussion

Figure 7.4 gives some results for each VFM analysis technique. When the inclusion is evident, the analyst must define the boundary. For the example shown in Fig. 7.4a, S_2 was defined as the region where $Q_{11} > 11.5$ GPa. In practice the analyst will likely choose many different boundaries and compare the identifications. Accurate identification of the maximum stiffness in this simulation is difficult; as the area of S_2 was reduced to a small region surrounding the peak stiffness, the identification was compromised due to lack of data, i.e., the amount of strain data.

Figure 7.4b shows some results of the EG analysis; each virtual element included 16 (4 × 4) strain measurements whose physical dimensions were 4.4 mm × 4.3 mm. An EG analysis provides equilibrium information at the center of the virtual element, so Fig. 7.4b is shorter and narrower by 1/2 the length and height of the EG virtual element. Pragmatic use of EG suggests that results of several sizes will be compared. The size chosen here was used to illustrate a potentially important result, namely the size of the inclusion. Because the EG element scanned within the inclusion, the results indicated the element was near equilibrium. Because Q_{11} and Q_{12} differed only a constant, 0.3 here, Q_{11} was effectively factored out of Eq. (7.7). Therefore, an EG analysis provides information on inclusion boundaries. If an inclusion is not physically apparent, an EG analysis can be used to locate inclusion boundaries which can, in turn, be used to create S_1 and S_2 regions for the VFM technique where location of the inclusion is known a priori.

Figure 7.4c provides example Fourier VFM results. In Eqs. (7.8) and (7.9), $N = 34$, giving total of 2449 coefficients ($a_{m,\,n}$, $b_{m,\,n}$) for Q_{11} alone. Results were smoothed with an 88 × 88 pixel smoothing filter and Q_{11} identification was denoted as NaN at the specimen edges. Because the grid simulated strains were 272 × 46 individual measurements, additional data were needed in order to determine the large number of coefficients. The grid strains were interpolated to 6000 × 1000 individual measurements and the limiting factor for the size of N was the amount of data in x_2 direction. Although data interpolation is not a best practice, its use here provided similar information of inclusion size and location, as did the EG analysis and can be similarly used to denote the inclusion boundary for the a priori VFM technique.

Finally, an infinite number of Q_{ij} parametrizations are possible, such as polynomial formulations, e.g., Devivier et al. [4]. Given the relatively small amount of data (272 × 46 matrix size for each ε_i) and, in this simulation, the small size of inclusion relative to the specimen dimensions, determination of the virtual displacements would lead to an ill-conditioned matrix needed for polynomial $Q_{i\,j}$ identification.

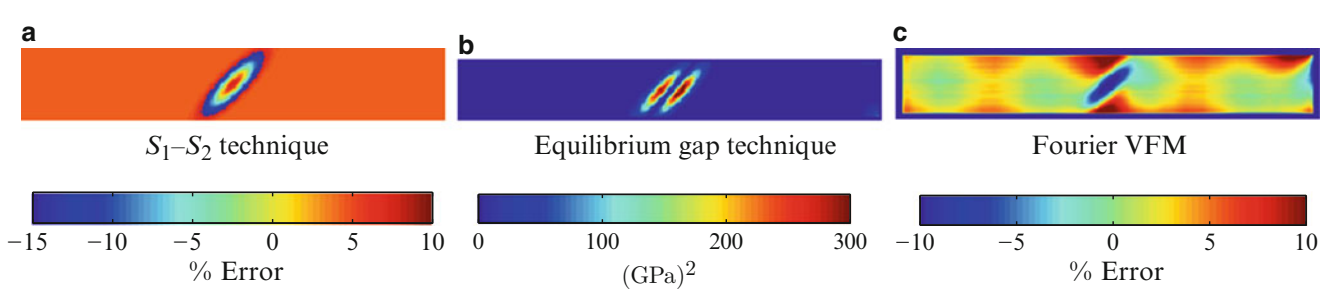

Fig. 7.4 Analysis results for each VFM technique. (**a**) S_1–S_2 technique. (**b**) Equilibrium gap technique. (**c**) Fourier VFM

7.5 Conclusion

Three VFM techniques were used to characterize the simulated, smoothly varying heterogeneous stiffness in a uniaxial tensile specimen. When the location of the inclusion was known, its stiffness could be identified within 10 % error; more accurate identification is possible with increased strain data density. Local equilibrium was examined and used to approximate inclusion size and location. Fourier VFM was used to provide inclusion location and size, but required significant data interpolation. Results of these three techniques suggest that their cooperative use could provide reasonable stiffness identification for heterogeneous materials using a uniaxial tensile test.

References

1. F. Pierron, M. Grédiac, *The Virtual Fields Method: Extracting Constitutive Mechanical Parameters from Full-Field Deformation Measurements* (Springer, New York, 2012)
2. M. Rossi, F. Pierron, On the use of simulated experiments in designing tests for material characterization from full-field measurements. Int. J. Solids Struct. **49**(3–4), 420–435 (2012)
3. J.M. Considine, Characterization of paper heterogeneity. PhD thesis, The University of Wisconsin-Madison (2014)
4. C. Devivier, F. Pierron, M.R. Wisnom, Impact damage detection in composite plates using deflectometry and the Virtual Fields Method. Compos. A Appl. Sci. **48**, 201–218 (2013)
5. P. Ladeveze, D. Leguillon, Error estimate procedure in the finite element method and applications. SIAM J. Numer. Anal. **20**(3), 485–509 (1983)
6. T.T. Nguyen, J.M. Huntley, I.A. Ashcroft, P.D. Ruiz, F. Pierron, A Fourier-series-based virtual fields method for the identification of 2-D stiffness distributions. Int. J. Numer. Methods Eng. **98**, 917–936 (2014)